Clinical Cancer Research

Genomic Profiling of Large-Cell Neuroendocrine Carcinoma of the Lung

Tomohiro Miyoshi[1,2,3], Shigeki Umemura[1,2], Yuki Matsumura[2], Sachiyo Mimaki[1], Satoshi Tada[1], Hideki Makinoshima[1], Genichiro Ishii[4], Hibiki Udagawa[1,2], Shingo Matsumoto[1,2], Kiyotaka Yoh[2], Seiji Niho[2], Hironobu Ohmatsu[2], Keiju Aokage[2], Tomoyuki Hishida[2], Junji Yoshida[2], Kanji Nagai[2], Koichi Goto[2], Masahiro Tsuboi[2], and Katsuya Tsuchihara[1]

Abstract

Purpose: Although large-cell neuroendocrine carcinoma (LCNEC) of the lung shares many clinical characteristics with small-cell lung cancer (SCLC), little is known about its molecular features. We analyzed lung LCNECs to identify biologically relevant genomic alterations.

Experimental Design: We performed targeted capture sequencing of all the coding exons of 244 cancer-related genes on 78 LCNEC samples [65 surgically resected cases, including 10 LCNECs combined with non–small cell lung cancer (NSCLC) types analyzed separately, and biopsies of 13 advanced cases]. Frequencies of genetic alterations were compared with those of 141 SCLCs (50 surgically resected cases and biopsies of 91 advanced cases).

Results: We found a relatively high prevalence of inactivating mutations in *TP53* (71%) and *RB1* (26%), but the mutation frequency in *RB1* was lower than that in SCLCs (40%, $P = 0.039$). In addition, genetic alterations in the PI3K/AKT/mTOR pathway were detected in 12 (15%) of the tumors: *PIK3CA* 3%, *PTEN* 4%, *AKT2* 4%, *RICTOR* 5%, and *mTOR* 1%. Other activating alterations were detected in *KRAS* (6%), *FGFR1* (5%), *KIT* (4%), *ERBB2* (4%), *HRAS* (1%), and *EGFR* (1%). Five of 10 cases of LCNECs combined with NSCLCs harbored previously reported driver gene alterations, all of which were shared between the two components. The median concordance rate of candidate somatic mutations between the two components was 71% (range, 60%–100%).

Conclusions: LCNECs have a similar genomic profile to SCLC, including promising therapeutic targets, such as the PI3K/AKT/mTOR pathway and other gene alterations. Sequencing-based molecular profiling is warranted in LCNEC for targeted therapies. *Clin Cancer Res; 23(3); 757–65. ©2016 AACR.*

Introduction

Large-cell neuroendocrine carcinoma (LCNEC) of the lung is a highly malignant tumor with a poor prognosis. It is a rare tumor, diagnosed in approximately 3% of patients with lung cancer who undergo surgical resection (1). LCNEC is classified as a neuroendocrine tumor along with small-cell lung cancer (SCLC) in the 4th edition of the *World Health Organization Classification of Lung Tumors* (2). LCNEC is distinguished from SCLC based on histologic criteria, including larger cell size, abundant cytoplasm, prominent nucleoli, vesicular nuclei or coarse chromatin, and a polygonal rather than a fusiform shape (3). Asamura and colleagues (4) demonstrated similar clinicopathologic characteristics and prognoses between 141 surgically resected LCNECs and 113 SCLCs in a large-scale Japanese multi-institutional study.

As LCNEC shares many similarities with SCLC in terms of histologic structure, immunohistochemical staining characteristics, and molecular biology (5–7), SCLC-based chemotherapy was expected to show similar effectiveness in patients with LCNEC (8). In a multicenter prospective phase II study, however, combination chemotherapy with irinotecan and cisplatin resulted in inferior overall survival (OS) among patients with LCNEC than those with SCLC (9), suggesting a metabolic distinction between LCNEC and SCLC.

Genomic analyses have revealed therapeutic targets in lung adenocarcinoma, such as *EGFR* mutations, and molecularly targeted therapies have achieved significant improvement in patient outcomes. Recent studies featuring comprehensive genomic analysis of SCLC have demonstrated a high prevalence of inactivating mutations in *TP53* and *RB1* (10–13). Genetic alterations in the PI3K/AKT/mTOR pathway were identified as possible therapeutic targets (12, 13). Because of its rarity, however, information about therapeutically relevant genetic alteration in LCNEC is insufficient.

In this report, we examined surgically resected LCNEC for biologically relevant genomic alterations using a next-generation sequencing–based genomic profiling analysis. Biopsied samples of advanced stage LCNEC, which are the major subject of molecular targeted therapies in clinical practice, were also analyzed to investigate the changes in genetic profiles with cancer progression.

[1]Exploratory Oncology Research and Clinical Trial Center, National Cancer Center, Chiba, Japan. [2]Department of Thoracic Oncology, National Cancer Center Hospital East, Chiba, Japan. [3]Department of Pathology, Keio University School of Medicine, Tokyo, Japan. [4]Division of Pathology, Exploratory Oncology Research and Clinical Trial Center, National Cancer Center, Chiba, Japan.

Note: Supplementary data for this article are available at Clinical Cancer Research Online (http://clincancerres.aacrjournals.org/).

Corresponding Author: Shigeki Umemura, Department of Thoracic Oncology, National Cancer Center Hospital East, 6-5-1 Kashiwanoha, Kashiwa, Chiba 277-8577, Japan. Phone: 814-7133-1111; Fax: 814-7131-4724; E-mail: sumemura@east.ncc.go.jp

doi: 10.1158/1078-0432.CCR-16-0355

Translational Relevance

Large-cell neuroendocrine carcinoma (LCNEC) of the lung, which has been histologically categorized as high-grade neuroendocrine carcinoma with small-cell lung cancer (SCLC), is a highly malignant tumor with a poor prognosis. Although targeted therapies might improve outcomes, little is known about the molecular features of LCNEC. In this study, sequencing-based molecular profiling of the largest number of Japanese patients with treatment-naïve LCNEC demonstrated that LCNEC had similar genomic profiles to SCLC, including promising therapeutic targets, such as the PI3K/AKT/mTOR pathway as well as other well-established activating alterations, such as *EGFR*, *ERBB2*, and *FGFR1*. Sequencing-based molecular profiling may identify patients that will benefit from novel targeted therapies in LCNEC. This is the first study to include LCNECs combined with other non–small cell lung cancer and demonstrate highly concordant genetic alterations, including key driver mutations, between each component. Agents targeted to these alterations would theoretically be effective for both components.

We compared the genomic profiles of LCNECs with those of SCLCs. Combined LCNECs with additional components of other non–small cell lung cancer (NSCLC) were analyzed for intratumoral heterogeneity to investigate the origin of LCNEC.

Materials and Methods

This study was approved by the Institutional Review Board (IRB) of the National Cancer Center, Japan (IRB number: 2011-201 and 2013-294). All clinicopathologic data extracted in this study were obtained from our database.

Samples

We collected 78 LCNEC samples (65 surgically resected and 13 biopsied from patients with advanced disease) from 1992 through 2014 and 90 advanced SCLC samples obtained by biopsy from 1995 through 2013 at the National Cancer Center Hospital East, Japan. All patients were chemotherapy naïve. All specimens had been fixed with 10% formalin (52 LCNECs and 90 SCLCs) or 100% methyl alcohol (26 LCNECs) and were embedded in paraffin. Serial 4-μm sections, including the largest diameter of the primary tumor, were stained using hematoxylin and eosin and were reviewed and classified by two pathologists (T. Miyoshi and G. Ishii) according to the 4th edition of the *World Health Organization Classification of Lung Tumors*. For LCNEC, neuroendocrine features were confirmed by at least one of the following neuroendocrine markers: CD56, chromogranin A, or synaptophysin. Specimens containing a minimum of 50% tumor cells were used for analysis.

We cored the tumor component out of the paraffin-embedded block with a 2-mm-diameter punch for tissue microarray (TMA) and used the core for DNA extraction. In cases of combined LCNEC and NSCLC, both components were identified using light microscopy and cored out separately. A representative example of LCNEC combined with adenocarcinoma is illustrated in Fig. 1, and histopathologic images of TMA cored out from each component (LCNEC and adenocarcinoma) are shown in Supplementary Fig. S1.

Procedures to extract DNA and target sequencing

DNA was prepared [Absolutely RNA FFPE Kit (modified protocol for DNA extraction), Agilent Technologies] and quantified (Quant-iT PicoGreen dsDNA Reagent and Kits, Life Technologies). Target-sequencing libraries were prepared using up to 1 μg of dsDNA. Targeted regions were captured using a custom target-capturing panel (SureSelect XT custom 0.5–2.9 Mb, Agilent Technologies) containing all the coding exons of 244 genes selected on

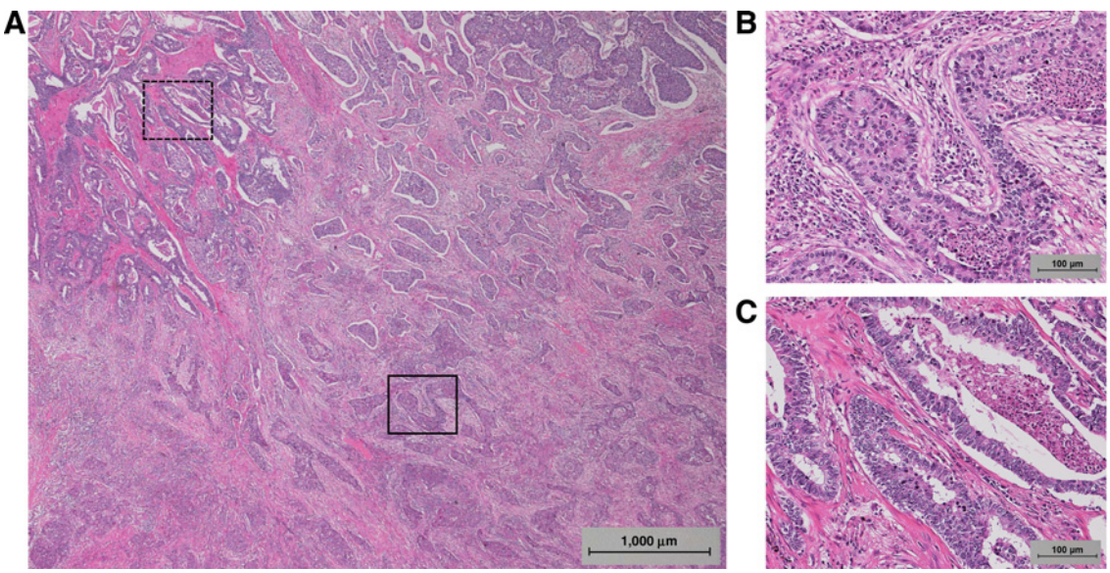

Figure 1.

A, Representative example of a combined LCNEC with adenocarcinoma (hematoxylin and eosin). Solid and dotted, LCNEC and adenocarcinoma components, respectively. **B,** LCNEC component: solid nest with peripheral palisading. **C,** Adenocarcinoma component: irregular glands with necrotic debris.

the basis of the results of previous genomic analyses of SCLC (Supplementary Table S1; ref. 12), giving a final capture size of 1.499 Mb. The target capture libraries were sequenced (HiSeq 1500, Illumina) to generate 100-bp paired-end data. The results of the sequencing run are shown in Supplementary Tables S2 and S3.

Mutation call

The sequencing reads were mapped to the UCSC human reference genome (GRCh37/hg19) using Burrows–Wheeler Aligner (BWA) software (14) set to the default parameters. The SNVs and insertions and deletions (indels) were called using the Genome Analysis Toolkit (GATK version 1.6, Broad Institute, Cambridge, MA; refs. 15, 16). Systematic errors in sequencing and mapping were filtered out using custom filters (GATK confidence score ≥ 50, number of variant reads in each direction ≥ 1, and variant allele frequency $\geq 10\%$). Known germline variations represented in the National Center for Biotechnology Information Database (dbSNP build 131; ref. 17) were excluded. In addition, rare germline SNVs were discarded using exomes provided from the 1000 Genomes Project (the phase I exome data, 20110521) and 274 in-house Japanese exomes. False-positive calls (residual errors after this filtering) were excluded through visual inspection. To reduce contamination of the germline variants as much as possible and to extract more probable variants as candidate somatic mutations, we defined candidate somatic mutations as follows: (i) nonsense, in-frame, and frame-shift insertions or deletions (indels); and (ii) missense mutations registered in the Catalogue of Somatic Mutations in Cancer (COSMIC, released ver. 72) database as "confirmed somatic" or "previously reported." We defined mutations with more than 10 cases registered in the COSMIC database as hotspot mutations.

Copy number analysis

We calculated the gene copy number using the total depth on the covered region of each 244 targeted genes. The copy number of a gene (gene: t) of a sample (sample: i) was defined as $C_{t,i}$, which was calculated as follows:

We defined "coverage rate" and calculated the coverage rate of gene t of a sample i ($R_{t,i}$) by dividing the total depth of gene t by the whole depth of the 244 genes in sample i:

$$R_{t,i} = \frac{\text{Total depth of gene t of sample i}}{\text{Total depth of the targeted 244 genes of sample i}} \quad \text{(A)}$$

The P values of the $R_{t,i}$ were calculated using the binomial probability function. We assumed the $R_{t,i}$ of gene t to be under $X \sim B(n, p)$. $X = \{\text{the integer of } nR_{t,i}\}$, setting $n = 1{,}000$ for convenience and $P = \text{mean}\{R_{t,i}\}$, respectively. Samples with P values of the $R_{t,i} < 0.05$ were excluded from calculation of the standard coverage rate of gene i ($R_{standard,\ i}$). If the number of samples whose P values of the $R_{t,i} \geq 0.05$ was m, $R_{standard,i}$ was calculated as follows:

$$R_{standard,i} = \frac{\sum_{k=1}^{m} R_{k,i}}{m} \quad \text{(B)}$$

The predicted copy number of gene t of a sample i ($C_{t,i}$) was calculated as follows:

$$C_{t,i} = 2 \times \frac{R_{t,i}}{R_{standard,i}} \quad \text{(C)}$$

The P values of the $C_{t,i}$ were also calculated using the binomial probability function.

We defined copy number gain if the $C_{t,i}$ was ≥ 4 and the P value of the $R_{t,i}$ was <0.05. Then, we defined copy number amplified if the $C_{t,i}$ was ≥ 10, and the P value of the $R_{t,i}$ was <0.05.

Comparison with SCLC

We performed target capture sequencing on 90 biopsy samples of advanced SCLC. The genomic alteration data for 50 surgically resected SCLC tumors and one advanced SCLC tumor (biopsied by mediastinoscopy) were extracted from our previous work (12). For SCLC cases with combined histology, only the SCLC component was selectively cored out and used for the analysis. Mutation call and copy number analyses were performed in the same manner as in the LCNEC samples. Combining genomic alteration data of these 141 SCLC samples, they were compared with the genomic profiles of the 78 LCNECs.

Validation of the result of target sequence and copy number analysis

We validated the accuracy of the results of the target sequencing employed in this study using a sequencing panel [Oncomine Cancer Research Panel (OCP), Fisher Scientific]. All 20 mutations detected in seven LCNEC mutations, and 13 SCLC mutations were validated with the OCP (Supplementary Table S4). We then performed Sanger sequencing for five mutations on the PI3K/AKT/mTOR pathway detected in LCNEC, and all of them were validated (Supplementary Fig. S2; Supplementary Tables S4 and S5). The methods of Sanger sequencing are summarized in the Supplementary Methods. In addition, one *EGFR* mutation (L858R) detected in a SCLC biopsy sample (No. 198) was validated by the PCR clamp method.

To validate the accuracy of copy number calculation using total depth on the covered region of each of the 244 targeted genes, we made a comparison with whole-exome sequencing for surgically resected SCLCs performed previously in our institution, in which an SNP array was employed to analyze the genotype and DNA copy number in 47 primary–normal paired samples.(12) In the SNP array, a gene was considered copy number amplified if the calculated copy number was ≥ 4. When we compared the results of the SNP array for surgically resected SCLC samples, the sensitivity, specificity, positive predictive value, and negative predictive value of the estimated copy number employed in this study were 43.6%, 99.9%, 85.0%, and 99.5%, respectively. Furthermore, we selected 10 genes in seven samples (four LCNEC samples and three SCLC biopsy samples) whose copy number was ≥ 4 and validated them using OCP. In OCP, a gene was considered as "amplification suspected" if the copy number obtained was ≥ 4 and "amplified" if the copy number obtained was ≥ 7. There was a high correlation between the estimated copy number calculated in this study and that obtained by OCP (Supplementary Fig. S3). In addition, we validated 13 samples (eight LCNEC samples, one SCLC biopsy sample, and four SCLC surgically resected samples), which had copy number gains in *MYCL1*, *MYC*, or *FGFR1* by a qPCR (Supplementary Fig. S4). The methods are summarized in the Supplementary Methods.

Eventually, all 18 copy number gains for *MYCL1*, *MYC*, or *FGFR1* subject to validation were confirmed via Oncomine and/or qPCR.

Immunohistochemical staining for ALK, RB, and p16

We performed immunohistochemical staining of ALK, RB, and p16 protein for all 65 resected LCNECs. The companies from which we purchased the antibodies and details of the IHC procedures are shown in Supplementary Table S6. The procedure for immunohistochemical staining of RB and p16 is summarized in the Supplementary Methods.

Statistical analysis

Differences in categorical variables between two groups for statistical significance were evaluated using the χ^2 test or Fisher exact test. All reported P values were two sided, and the significance level was set at $P < 0.05$. Analyses were performed using commercial software (SPSS 22 SPSS II for Windows, SPSS Inc.).

Results

Patient demographics

Demographics of the 78 patients with LCNEC are summarized in Table 1. Median age at the time of surgical resection or biopsy was 70 years (range, 22–84). Sixty-seven (86%) patients were male, and 76 (97%) patients had a history of smoking. Pathologic stages were distributed as follows: I/II/III = 38/14/13 for 65 surgically resected patients, and clinical stages were distributed as follows: II/III/IV = 1/4/8 for 13 advanced biopsy patients.

For the 91 SCLC biopsy cases, median age at the time of biopsy was 67 years (range, 37–85). Seventy-one (78%) patients were male, and 88 (97%) patients had a history of smoking. Clinical stages were distributed as follows: II/III/IV = 1/26/64.

Frequent genetic alterations and comparison between LCNEC and SCLC

The profile of frequent genetic alterations in LCNECs and SCLCs is in Fig. 2, and the entire list of mutations is provided in the

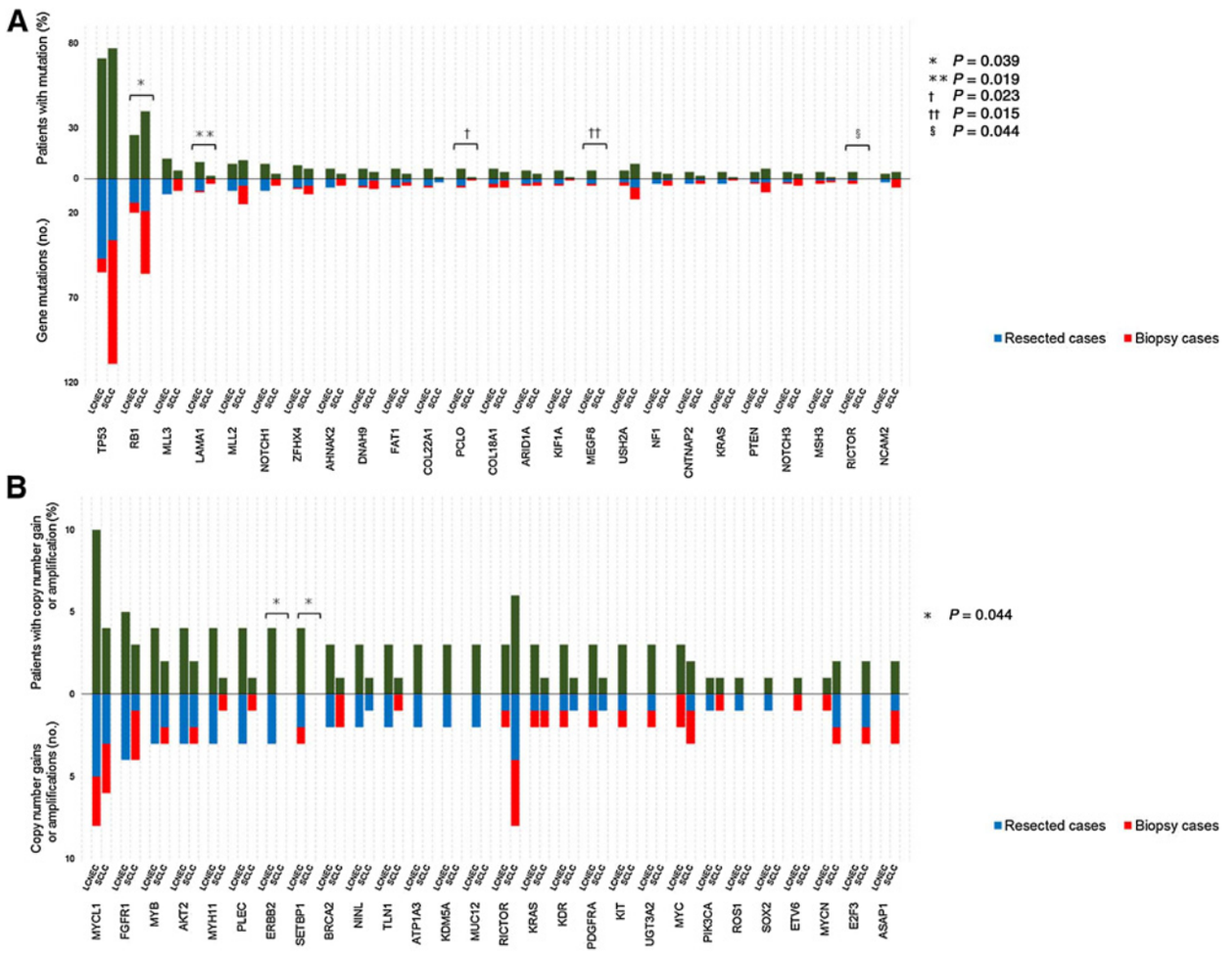

Figure 2.

Profile of frequent genetic alterations in LCNEC compared with SCLC. **A,** The mutation frequency of *RB1* in LCNECs (20 cases, 26%) was lower than that in the SCLCs (40%, $P = 0.039$). The mutations of *LAMA1, PCLO, MEGF8*, and *RICTOR* were significantly more frequent in LCNEC than SCLC. **B,** Copy number gains or amplifications of *ERBB2* and *SETBP1* were significantly more frequent in LCNEC than SCLC.

Figure 3.

Overview of key driver mutations and other activating mutations in LCNEC of the lung. Genetic alterations in the PI3K/AKT/mTOR pathway were detected in 12 (15%) tumors. Copy number gains of *MYC* family member occurred in 11 (14%) of the tumors, and copy number gains of each *MYC* family member were mutually exclusive. Other genetic alterations were detected in *KRAS* (6%), *FGFR1* (5%), *KIT* (4%), *ERBB2* (4%), *HRAS* (1%), and *EGFR* (1%).

Supplementary Tables S7 and S8. In all LCNECs, both resected and biopsy cases, we identified a relatively high prevalence of inactivating mutations in *TP53* (55 cases, 71%) and *RB1* (20 cases, 26%). The mutation frequency of *RB1* in the LCNECs was lower than that in the SCLCs (40%, $P = 0.039$). Other mutations that were significantly more frequent in LCNEC were as follows: *LAMA1* (10% in LCNEC and 2% in SCLC, $P = 0.019$), *PCLO* (6% in LCNEC and 1% in SCLC, $P = 0.023$), *MEGF8* (5% in LCNEC and 0% in SCLC, $P = 0.015$), and *RICTOR* (3% in LCNEC and 0% in SCLC, $P = 0.044$). Copy number gain in *ERBB2* and *SETBP1* was significantly more frequent in LCNEC (4% in LCNEC and 0% in SCLC, $P = 0.044$).

Comparison between resected and biopsy cases

In LCNEC, the number of patients with copy number gain in *MYC* family genes was significantly higher in advanced stage biopsy cases (*MYC*/*MYCL1*/*MYCN*, 15%/23%/8%) than in early-stage surgically resected cases (*MYC*/*MYCL1*/*MYCN*, 0%/8%/0%; $P = 0.002$). Other genomic alterations did not differ among disease stages.

Key driver mutations

As for key driver mutations, we focused on the mutations that occurred in the receptor tyrosine kinases (RTK)/RAS signaling pathway genes listed in two previous comprehensive genomic studies of lung cancer (13, 18). An overview of the key driver alterations and other activating alterations in LCNEC is shown in Fig 3. Genetic mutations or copy number gains in the PI3K/AKT/mTOR pathway were detected in 12 (15%) of the tumors: *PIK3CA* (3%), *PTEN* (4%), *AKT2* (4%), *RICTOR* (5%), and *mTOR* (1%). Amplifications of each *MYC* family gene were mutually exclusive.

Other activating alterations were detected in *KRAS* (6%), *FGFR1* (5%), *KIT* (4%), *ERBB2* (4%), *HRAS* (1%), and *EGFR* (1%). Among the 18 cases with mutations in targetable RTK genes, three cases had an activating mutation in the protein tyrosine kinase domain: one in *EGFR* (E746_A750 del), one in *KIT* (D816H), and one in *ERBB2* (V842I). Hotspot mutations detected in this study are listed in Table 2.

For the 141 SCLC patients, including surgically resected and biopsy cases, Supplementary Fig. S5 shows an overview of the key driver alterations and other activating alterations. Genetic alterations in the PI3K/AKT/mTOR pathway were detected in 24 (17%) of the tumors: *PIK3CA* (4%), *PTEN* (6%), *AKT2* (2%), and *RICTOR* (6%). Other known activating alterations were also detected in *FGFR1* (3%), *KRAS* (2%), *KIT* (1%), *ERBB2* (1%), and *EGFR* (1%). Among 91 biopsy cases, genetic alterations in the

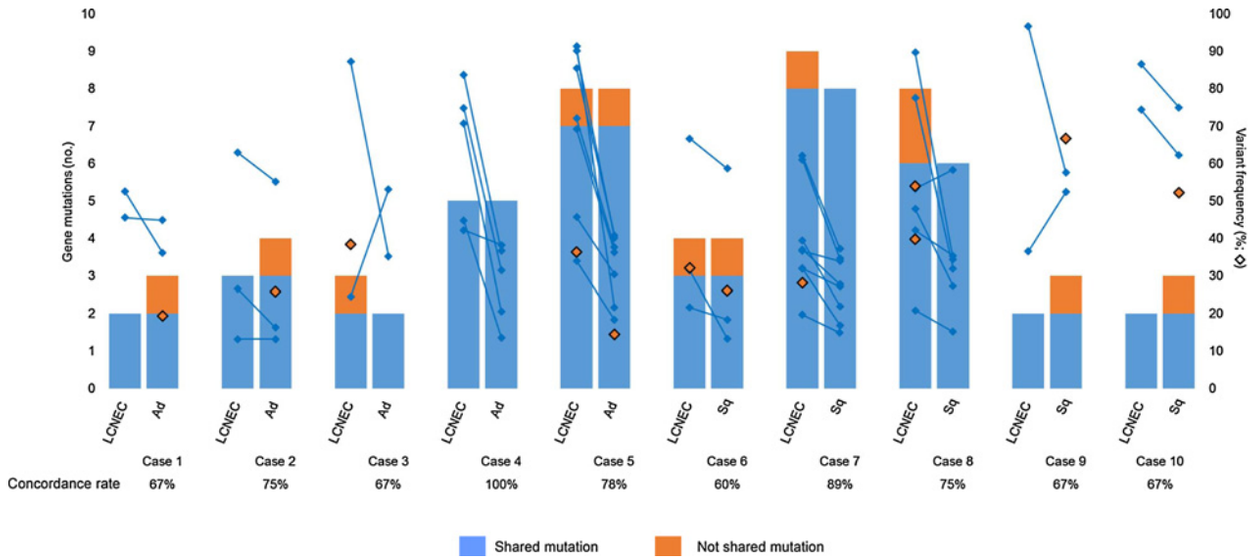

Figure 4.
Number of genetic mutations and variant frequency of each gene in 10 combined LCNECs. Variant frequency of mutations in the NSCLC component tended to be lower than those shared with the LCNEC component. We suppose that the tumor contents in the NSCLC component were generally less than that in LCNEC component as illustrated in Supplementary Fig. S1.

PI3K/AKT/mTOR pathway were detected in 15 (16%) of the tumors: *PIK3CA* (4%), *PTEN* (7%), *AKT2* (1%), and *RICTOR* (4%). Other activating alterations were also detected in *FGFR1* (3%), *KRAS* (2%), *KIT* (1%), and *EGFR* (1%). Hotspot mutations detected in the biopsy cases of SCLC are listed in the Supplementary Table S9.

Immunohistochemical staining for ALK, RB1, and p16

In the 65 resected LCNECs, no sample was positive for ALK staining, suggesting that these cases did not possess any fusion of this gene. Decreased expression of RB protein was detected in 74% (48/65) of the samples by IHC. Most of the *RB1*-mutated samples (93%, 13/14) were negative for RB staining, and the mutual exclusivity of protein expression between RB and p16 was distinct (Supplementary Fig. S6).

Table 1 . Patient characteristics

Characteristic	No. of patients LCNEC ($n = 78$)	SCLC ($n = 141$)
Gender: male/female	67/11	113/28
Age, years: median (range)	70 (22–84)	67 (37–86)
Smoking status: never/ever	2/76	3/138
Pack years: median (range)	51 (0–208)	50 (0–164)
Histology: pure/combined type	68/10	129/12
Surgically resected/biopsy	65/13	51/90
Surgically resected sample	65	50
Pathologic stage I/II/III	38/14/13	28/13/9
Vascular invasion: present/absent	52/13	42/8
Lymphatic invasion: present/absent/unknown	23/42/0	18/31/1
Pleural invasion: present/absent/unknown	25/40/0	19/31
Biopsy sample	13	91
Clinical stage II/III/IV	1/4/8	1/26/64
Biopsy procedure: TBLB/ lymph node biopsy/others	9/2/2	63/8/20
First-line treatment: CRT/ chemotherapy alone/RT alone BSC unknown	4/7/1/1	23/65/2/1

Abbreviations: BSC, best supportive care; CRT, chemoradiotherapy; RT, radiotherapy; TBLB, transbronchial lung biopsy.

Relationship between genomic alteration of RTKs and protein expression in LCNEC

Supplementary Fig. S7 shows the relationship between RTK overexpression and genomic alterations in 51 resected LCNECs. The protein expression data for these LCNEC tumors are from our previous report (7). In this analysis, we saw no significant correlation between strong positivity for RTK expression and genomic alterations.

Overall survival of surgically resected LCNEC cases

The median follow-up period was 37 months. The 3-year OS rate for the 65 surgically resected LCNEC patients was 65%. We classified cases with/without PI3K/AKT/mTOR pathway alteration, copy number gain in MYC family genes, RB expression, and p16 expression, but no prognostic significance was determined (data not shown).

Combined LCNEC

In one case of LCNEC combined with adenocarcinoma, both components shared a well-established in-frame deletion in *EGFR*: protein tyrosine kinase domain in Exon 19 (E746_A750 del). A case of LCNEC combined with adenocarcinoma had an activating mutation in *KRAS*: ras family domain in codon 12 (G12V) in both components, and one LCNEC combined with squamous cell carcinoma (SCC) had an activating mutation in *PIK3CA*: the catalytic subunit of phosphoinositide-3 kinase (E545K) in both components. In total, five of 10 LCNECs combined with another tumor type harbored the same key driver mutations in both components. An overview of the individual mutations occurring in each component is listed

Table 2. Hotspot mutations detected in LCNEC

Symbol	Case No.	Mutation type	Mutation site
PIK3CA	LCNEC_68c	E545K	*PI3K* helical domain
KRAS	LCNEC_39c	G12D	Ras family domain
	LCNEC_62c	G12V	Ras family domain
	LCNEC_46c	Q61R	Ras family domain
HRAS	LCNEC_1c	G13V	Ras family domain
KIT	LCNEC_26c	D816H	Protein tyrosine kinase domain
ERBB2	LCNEC_40c	V842I	Protein tyrosine kinase domain
EGFR	LCNEC_60c	E746_A750 del	Protein tyrosine kinase domain

in Table 3 and in Supplementary Table S10. One LCNEC with SCC had copy number gain in *FGFR1*.

The median number of genetic mutations in the 10 combined LCNECs was 3.5 (range, 2–9) in the LCNEC component and 4 (range, 2–8) in the NSCLC component (Fig. 4). The concordance rate was calculated by dividing the number of common genetic mutations by the total number of genetic alterations of the two components. In this study, the median concordance rate between LCNEC and associated NSCLC components was 71% (range, 60–100%).

Discussion

In this sequencing-based molecular profiling of Japanese patients with chemotherapy-naïve LCNEC in comparison with SCLC, we found that LCNEC and SCLC had similar genomic profiles, including promising therapeutic targets, such as the PI3K/AKT/mTOR pathway. LCNEC harbored other targetable activating mutations, such as *EGFR*, *ERBB2*, and *FGFR1*. To our knowledge, this is the first study to include combined LCNECs and analyze each histologic component separately. Agents targeted to these alterations would theoretically be effective for both components.

Genetic alterations in the PI3K/AKT/mTOR pathway were detected in 15% of LCNECs. This pathway may play a critical role in LCNEC tumorigenesis. Genetic alterations in this pathway have been noted as a promising therapeutic target in SCLC (12, 19–23), and targeted therapy for this pathway may also be promising in LCNEC. Mutual exclusiveness was observed in the copy number gain of each *MYC* family gene. This suggests the possibility that *MYC* family genes are driver oncogenes in LCNEC and that this gene group may also be therapeutic targets.

We also revealed that LCNEC has activating mutations in RTK genes, such as *EGFR*, *KIT*, and *ERBB2*. *EGFR* exon 19 deletion (E746_A750 del) is known to be associated with high sensitivity to EGFR tyrosine kinase inhibitors (TKI). This case with an *EGFR* mutation was of combined LCNEC with adenocarcinoma. Immunohistochemical staining of this case revealed protein expression of EGFR in both LCNEC and adenocarcinoma components. Although this case did not receive target therapy, EGFR-TKIs, as reported by Niederst and colleagues (24), might be effective. *ERBB2* mutation in the protein tyrosine kinase domain (V842I) was reported to be the spot associated with sensitivity to the irreversible kinase inhibitor neratinib (25). Amplified *FGFR1* is also a promising therapeutic target (26). Clinical trials to test possible agents targeted to these mutations are warranted in this disease. Biomarker-based patient selection will be necessary for optimal efficacy.

In this study, we revealed a discrepancy between the genetic alteration and expression of RTK in LCNEC. This may be because protein overexpression of RTK is not directly caused by gene amplification and/or mutation. For instance, the overexpression of c-KIT is frequently observed in high-grade neuroendocrine carcinoma (HGNEC; refs. 7, 27–29), but three previous trials of imatinib failed to show a response in SCLC (30–32). This result was explained as due to the rarity of activating *c-KIT* mutations in SCLC.

The high frequency of mutation of *TP53* (71%) and *RB1* (26%) in LCNEC also suggests the characteristics of HGNEC. Recently, a high prevalence of inactivating mutations in tumor suppressor genes *TP53* and *RB1*, amplification of *MYC* family members, and mutation of histone modifiers (*CREBBP* and *EP300*) has been highlighted in SCLC by whole-exome sequencing. According to these reports, the prevalence of genetic alterations is 80% to 89% in *TP53* and 39% to 67% in *RB1* (10–12, 33). Suzuki and colleagues (34) reported that the mutation frequency of *TP53* and *RB1* in 97 Japanese patients with adenocarcinoma was only 23% and 1%, respectively. In contrast, the mutation frequency of *RB1* (26%) in LCNEC in this study was high and similar to that revealed in a previous whole-exome sequencing study of 15 LCNECs (30%; ref. 35). Recently, Rekhtman and colleagues performed next-generation sequencing of 45 LCNEC samples and reported a frequency of *RB1* mutation, loss of *RB1*, and protein loss of RB was 14 (31%), 3 (7%), and 18 (40%), respectively, suggesting that copy number loss and other molecular events, such as epigenomic modulations, might contribute to the functional impairment of RB proteins (36). Therefore, we additionally evaluated RB protein expression and found that protein loss of RB occurred in up to 74% of cases. In addition, we confirmed the distinct exclusivity between RB and p16 in LCNEC, suggesting the biological importance of the RB/p16 pathway in LCNEC tumorigenesis, as reported in previous studies for NSCLC (37, 38). Although the frequency was significantly lower than that of SCLC in this study, the relatively high mutation frequency of *TP53* and *RB1* in LCNEC suggests the similarity of LCNEC to SCLC.

Table 3. Overview of individual mutations in each component of 10 LCNECs combined with another cell type

	LCNEC combined with adenocarcinoma										LCNEC combined with SCC									
	Case 1		Case 2		Case 3		Case 4		Case 5		Case 6		Case 7		Case 8		Case 9		Case 10	
Symbol	L	A (pap)	L	A (aci)	L	A (aci)	L	A (pap)	L	A (aci)	L	S	L	S	L	S	L	S	L	S
Mutation																				
TP53	H214R		E258G				K120E		R283P				R158L		N131Y		E285*		V157F	
RB1					W99*						R579*									
PIK3CA													E545K							
KRAS							G12V													
EGFR					E746_A750 del															
IGF1R									G870*											
MET																	V1088M			

Abbreviations: A, adenocarcinoma component; aci, acinar adenocarcinoma; L, LCNEC component; pap, papillary adenocarcinoma; S, SCC component.

To further analyze the relationship between LCNEC and SCLC, we performed a Search Tool for the Retrieval of Interacting Genes/Proteins (STRING) analysis using the STRING database (http://string-db.org/). The protein–protein interaction networks were obtained by applying the six most frequently mutated genes (*TP53*, *RB1*, *MLL3*, *LAMA1*, *MLL2*, and *NOTCH1*). The STRING network enrichment results on KEGG pathways indicated a strong association with pathways of SCLC ($P = 0.00038$; Supplementary Table S11).

LAMA1, *PCLO*, *MEGF8*, and *RICTOR* were more mutated in LCNECs than with SCLC. It is reported that *LAMA1* is associated with cancer pathways, such as integrin signaling and cell adhesion in NSCLC (39). In addition, *PCLO* promoted cell invasion in liver cancer cell lines (40). These four genes might be associated with the etiology of LCNEC; however, confirmation in large studies is needed, and functional experiments on these genes are required to clarify their biological role.

Patient backgrounds show that most of the biopsy cases were of advanced disease. On comparison of the resected cases and biopsy cases, copy number gain in *MYC* family genes was significantly more frequent in advanced cases of LCNEC. Amplified *MYC* family genes are reported to be negative prognostic factors in lung SCLC (41), and this may also apply to LCNEC.

In LCNECs combined with adenocarcinoma, two pairs had well-established oncogenic mutations (one in *EGFR* and one in *KRAS*), while in LCNEC combined with SCC, one pair had a *PIK3CA*-activating mutation and one pair had copy number gain in *FGFR1*. In total, up to half of the combined LCNECs had established key driver mutations in both components, suggesting that therapies targeted toward these alterations would be effective for combined LCNECs. These genetic alterations were shared in both LCNEC and NSCLC components. In addition, both components also shared genetic alterations of *TP53* or *RB1*. These shared driver mutations between LCNEC and NSCLC components suggest that these mutations were acquired relatively early in the evolution of the combined LCNEC. In this study, the median concordance rate of genetic alterations in combined LCNEC was 71%. Zhang and colleagues (42) investigated the intratumoral heterogeneity in 11 localized lung adenocarcinomas by multi-region whole-exome sequencing and reported that 76% of all mutations and 20 of 21 known cancer gene mutations were identified in all regions of individual tumors. These concordance rates are similar, suggesting that the concordance rate of combined LCNEC is relatively high despite the morphologic differences between LCNEC and NSCLC. Further investigation is needed.

In conclusion, LCNEC and SCLC, which have been histologically categorized as HGNEC, have similar genomic profiles, including promising therapeutic targets, such as the PI3K/AKT/mTOR pathway. LCNEC harbored other targetable activating mutations, including *EGFR*, *ERBB2*, and *FGFR1*. Sequencing-based molecular profiling may identify patients that will benefit from novel targeted therapies. In combined LCNECs, LCNEC and NSCLC components had highly concordant genetic alterations, including key driver mutations, despite their distinct morphologic appearances. Agents targeted to these alterations would theoretically be effective for both components.

Disclosure of Potential Conflicts of Interest

No potential conflicts of interest were disclosed.

Authors' Contributions

Conception and design: T. Miyoshi, S. Umemura, S. Matsumoto, S. Niho, K. Goto, M. Tsuboi, K. Tsuchihara

Development of methodology: T. Miyoshi, S. Umemura, S. Tada, H. Makinoshima, S. Matsumoto, K. Goto, K. Tsuchihara

Acquisition of data (provided animals, acquired and managed patients, provided facilities, etc.): T. Miyoshi, S. Umemura, Y. Matsumura, S. Mimaki, H. Makinoshima, G. Ishii, S. Niho, H. Ohmatsu, K. Tsuchihara

Analysis and interpretation of data (e.g., statistical analysis, biostatistics, computational analysis): T. Miyoshi, S. Umemura, S. Tada, H. Makinoshima, H. Udagawa, J. Yoshida, K. Tsuchihara

Writing, review, and/or revision of the manuscript: T. Miyoshi, S. Umemura, G. Ishii, H. Udagawa, K. Yoh, K. Aokage, T. Hishida, J. Yoshida, K. Nagai, K. Goto, M. Tsuboi, K. Tsuchihara

Administrative, technical, or material support (i.e., reporting or organizing data, constructing databases): T. Miyoshi, S. Umemura, S. Tada, H. Makinoshima, S. Matsumoto, K. Tsuchihara

Study supervision: T. Miyoshi, S. Umemura, S. Niho, K. Aokage, K. Nagai, K. Goto, K. Tsuchihara

Other (pathologic examination): G. Ishii

Grant Support

This study was performed as a research program of the Project for Development of Innovative Research on Cancer Therapeutics (P-Direct), Japan Agency for Medical Research and Development (AMED), and was supported by JSPS KAKENHI grant numbers 24300346 and 26870876 and the National Cancer Center Research and Development Fund (25-A-6).

The costs of publication of this article were defrayed in part by the payment of page charges. This article must therefore be hereby marked *advertisement* in accordance with 18 U.S.C. Section 1734 solely to indicate this fact.

Received February 8, 2016; revised July 20, 2016; accepted July 29, 2016; published OnlineFirst August 9, 2016.

References

1. Takei H, Asamura H, Maeshima A, Suzuki K, Kondo H, Niki T, et al. Large cell neuroendocrine carcinoma of the lung: a clinicopathologic study of eighty-seven cases. J Thorac Cardiovasc Surg 2002;124:285–92.
2. World Health Organization Classification of Tumours. Pathology and genetics: tumours of the lung, pleura, thymus and heart. Travis WD, Brambilla E, Burke AP, editors. Geneva, Switzerland: World Health Organization; 2015.
3. Battafarano RJ, Fernandez FG, Ritter J, Meyers BF, Guthrie TJ, Cooper JD, et al. Large cell neuroendocrine carcinoma: an aggressive form of non-small cell lung cancer. J Thorac Cardiovasc Surg 2005;130:166–72.
4. Asamura H, Kameya T, Matsuno Y, Noguchi M, Tada H, Ishikawa Y, et al. Neuroendocrine neoplasms of the lung: a prognostic spectrum. J Clin Oncol 2006;24:70–6.
5. Jones MH, Virtanen C, Honjoh D, Miyoshi T, Satoh Y, Okumura S, et al. Two prognostically significant subtypes of high-grade lung neuroendocrine tumours independent of small-cell and large-cell neuroendocrine carcinomas identified by gene expression profiles. Lancet 2004;363:775–81.
6. Cerilli LA, Ritter JH, Mills SE, Wick MR. Neuroendocrine neoplasms of the lung. Am J Clin Pathol 2001;116:S65–96.
7. Matsumura Y, Umemura S, Ishii G, Tsuta K, Matsumoto S, Aokage K, et al. Expression profiling of receptor tyrosine kinases in high-grade neuroendocrine carcinoma of the lung: a comparative analysis with adenocarcinoma and squamous cell carcinoma. J Cancer Res Clin Oncol 2015;141:2159–70.
8. Le Treut J, Sault MC, Lena H, Souquet PJ, Vergnenegre A, Le Caer H, et al. Multicentre phase II study of cisplatin-etoposide chemotherapy for

advanced large-cell neuroendocrine lung carcinoma: the GFPC 0302 study. Ann Oncol 2013;24:1548–52.
9. Niho S, Kenmotsu H, Sekine I, Ishii G, Ishikawa Y, Noguchi M, et al. Combination chemotherapy with irinotecan and cisplatin for large-cell neuroendocrine carcinoma of the lung: a multicenter phase II study. J Thorac Oncol 2013;8:980–4.
10. Rudin CM, Durinck S, Stawiski EW, Poirier JT, Modrusan Z, Shames DS, et al. Comprehensive genomic analysis identifies SOX2 as a frequently amplified gene in small-cell lung cancer. Nat Genet 2012;44:1111–6.
11. Peifer M, Fernandez-Cuesta L, Sos ML, George J, Seidel D, Kasper LH, et al. Integrative genome analyses identify key somatic driver mutations of small-cell lung cancer. Nat Genet 2012;44:1104–10.
12. Umemura S, Mimaki S, Makinoshima H, Tada S, Ishii G, Ohmatsu H, et al. Therapeutic priority of the PI3K/AKT/mTOR pathway in small cell lung cancers as revealed by a comprehensive genomic analysis. J Thorac Oncol 2014;9:1324–31.
13. George J, Lim JS, Jang SJ, Cun Y, Ozretic L, Kong G, et al. Comprehensive genomic profiles of small cell lung cancer. Nature 2015;524:47–53.
14. Li H, Durbin R. Fast and accurate short read alignment with Burrows-Wheeler transform. Bioinformatics 2009;25:1754–60.
15. McKenna A, Hanna M, Banks E, Sivachenko A, Cibulskis K, Kernytsky A, et al. The Genome Analysis Toolkit: a MapReduce framework for analyzing next-generation DNA sequencing data. Genome Res 2010;20: 1297–303.
16. DePristo MA, Banks E, Poplin R, Garimella KV, Maguire JR, Hartl C, et al. A framework for variation discovery and genotyping using next-generation DNA sequencing data. Nat Genet 2011;43:491–8.
17. Sherry ST, Ward MH, Kholodov M, Baker J, Phan L, Smigielski EM, et al. dbSNP: the NCBI database of genetic variation. Nucleic Acids Res 2001; 29:308–11.
18. The Cancer Genome Atlas Research Network. Comprehensive genomic characterization of squamous cell lung cancers. Nature 2012;489:519–25.
19. Wakuda K, Kenmotsu H, Serizawa M, Koh Y, Isaka M, Takahashi S, et al. Molecular profiling of small cell lung cancer in a Japanese cohort. Lung Cancer 2014;84:139–44.
20. Voortman J, Lee JH, Killian JK, Suuriniemi M, Wang Y, Lucchi M, et al. Array comparative genomic hybridization-based characterization of genetic alterations in pulmonary neuroendocrine tumors. Proc Natl Acad Sci U S A 2010;107:13040–5.
21. Wojtalla A, Fischer B, Kotelevets N, Mauri FA, Sobek J, Rehrauer H, et al. Targeting the phosphoinositide 3-kinase p110-alpha isoform impairs cell proliferation, survival, and tumor growth in small cell lung cancer. Clin Cancer Res 2013;19:96–105.
22. Shibata T, Kokubu A, Tsuta K, Hirohashi S. Oncogenic mutation of PIK3CA in small cell lung carcinoma: a potential therapeutic target pathway for chemotherapy-resistant lung cancer. Cancer Lett 2009; 283:203–11.
23. Marinov M, Ziogas A, Pardo OE, Tan LT, Dhillon T, Mauri FA, et al. AKT/mTOR pathway activation and BCL-2 family proteins modulate the sensitivity of human small cell lung cancer cells to RAD001. Clin Cancer Res 2009;15:1277–87.
24. Niederst MJ, Sequist LV, Poirier JT, Mermel CH, Lockerman EL, Garcia AR, et al. RB loss in resistant EGFR mutant lung adenocarcinomas that transform to small-cell lung cancer. Nat Commun 2015;6:6377.
25. Bose R, Kavuri SM, Searleman AC, Shen W, Shen D, Koboldt DC, et al. Activating HER2 mutations in HER2 gene amplification negative breast cancer. Cancer Discov. 2013;3:224–37.
26. Thomas A, Lee JH, Abdullaev Z, Park KS, Pineda M, Saidkhodjaeva L, et al. Characterization of fibroblast growth factor receptor 1 in small-cell lung cancer. J Thorac Oncol 2014;9:567–71.
27. Lu HY, Zhang G, Cheng QY, Chen B, Cai JF, Wang XJ, et al. Expression and mutation of the c-kit gene and correlation with prognosis of small cell lung cancer. Oncol Lett 2012;4:89–93.
28. Schneider BJ, Kalemkerian GP, Ramnath N, Kraut MJ, Wozniak AJ, Worden FP, et al. Phase II trial of imatinib maintenance therapy after irinotecan and cisplatin in patients with c-Kit-positive, extensive-stage small-cell lung cancer. Clin Lung Cancer 2010;11:223–7.
29. Araki K, Ishii G, Yokose T, Nagai K, Funai K, Kodama K, et al. Frequent overexpression of the c-kit protein in large cell neuroendocrine carcinoma of the lung. Lung Cancer 2003;40:173–80.
30. Dy GK, Miller AA, Mandrekar SJ, Aubry MC, Langdon RMJr, Morton RF, et al. A phase II trial of imatinib (ST1571) in patients with c-kit expressing relapsed small-cell lung cancer: a CALGB and NCCTG study. Ann Oncol 2005;16:1811–6.
31. Johnson BE, Fischer T, Fischer B, Dunlop D, Rischin D, Silberman S, et al. Phase II study of imatinib in patients with small cell lung cancer. Clin Cancer Res 2003;9:5880–7.
32. Krug LM, Crapanzano JP, Azzoli CG, Miller VA, Rizvi N, Gomez J, et al. Imatinib mesylate lacks activity in small cell lung carcinoma expressing c-kit protein: a phase II clinical trial. Cancer 2005;103:2128–31.
33. Ross JS, Wang K, Elkadi OR, Tarasen A, Foulke L, Sheehan CE, et al. Next-generation sequencing reveals frequent consistent genomic alterations in small cell undifferentiated lung cancer. J Clin Pathol 2014;67:772–6.
34. Suzuki A, Mimaki S, Yamane Y, Kawase A, Matsushima K, Suzuki M, et al. Identification and characterization of cancer mutations in Japanese lung adenocarcinoma without sequencing of normal tissue counterparts. PLoS One 2013;8:e73484.
35. The Clinical Lung Cancer Genome Project (CLCGP); Network Genomic Medicine (NGM). A genomics-based classification of human lung tumors. Sci Transl Med 2013;5:209ra153.
36. Rekhtman N, Pietanza MC, Hellmann MD, Naidoo J, Arora A, Won H, et al. Next-generation sequencing of pulmonary large cell neuroendocrine carcinoma reveals small cell carcinoma-like and non-small cell carcinoma-like subsets. Clin Cancer Res 2016;22:3618–29.
37. Kashiwabara K, Oyama T, Sano T, Fukuda T, Nakajima T. Correlation between methylation status of the p16/CDKN2 gene and the expression of p16 and Rb proteins in primary non-small cell lung cancers. Int J Cancer 1998;79:215–20.
38. Sakaguchi M, Fujii Y, Hirabayashi H, Yoon HE, Komoto Y, Oue T, et al. Inversely correlated expression of p16 and Rb protein in non-small cell lung cancers: an immunohistochemical study. Int J Cancer 1996;65:442–5.
39. Xiong D, Li G, Li K, Xu Q, Pan Z, Ding F, et al. Exome sequencing identifies MXRA5 as a novel cancer gene frequently mutated in non-small cell lung carcinoma from Chinese patients. Carcinogenesis 2012;33:1797–805.
40. Fujimoto A, Furuta M, Shiraishi Y, Gotoh K, Kawakami Y, Arihiro K, et al. Whole-genome mutational landscape of liver cancers displaying biliary phenotype reveals hepatitis impact and molecular diversity. Nat Commun 2015;6:6120.
41. Alves Rde C, Meurer RT, Roehe AV. MYC amplification is associated with poor survival in small cell lung cancer: a chromogenic in situ hybridization study. J Cancer Res Clin Oncol 2014;140:2021–5.
42. Zhang J, Fujimoto J, Zhang J, Wedge DC, Song X, Zhang J, et al. Intratumor heterogeneity in localized lung adenocarcinomas delineated by multi-region sequencing. Science 2014;346:256–9.